Spin-density distribution in the copper site of azurin

Fittipaldi, M.; Warmerdam, G.C.M.; Waal, E.C. de; Canters, G.W.; Cavazzini, D.; Rossi, G.; ... ; Groenen, E.J.J.

CHEMPHYSCHEM

DOI: 10.1002/cphc.200500551

Spin-Density Distribution in the Copper Site of Azurin

Maria Fittipaldi,[a] Gertrud C. M Warmerdam,[b] Ellen C. de Waal,[b] Gerard W. Canters,[b] Davide Cavazzini,[c] Gian Luigi Rossi,[c] Martina Huber,[a] and Edgar J. J. Groenen*[a]

A 95 GHz pulsed deuterium ENDOR study has been performed on single crystals of azurin from Pseudomonas aeruginosa *selectively deuterated at the C_β position of the copper-coordinating cysteine 112. Complete hyperfine tensors of the two deuterium atoms have been obtained, which reveal identical isotropic parts. Analysis of the hyperfine tensors provides insight into the spin-density delocalization over the cysteine ligand. Approximately 45% of the spin density in the paramagnetic site can be attributed to copper and 30% to sulfur.*

Introduction

Blue-copper proteins such as azurin are involved in the electron-transfer chain of bacteria. In such proteins the redox-active center consists of a copper ion, which is invariably coordinated by three strong equatorial ligands—the sulfur atom S_γ of a cysteine residue and the nitrogen atoms N_δ of two histidine residues—and a weaker axial ligand, commonly the sulfur atom S_γ of a methionine residue. The center is embedded in the protein, and understanding electron acceptance from and electron donation to its reaction partners requires detailed insight into the electronic structure of these proteins, in particular of their copper sites. From the viewpoint of copper coordination the blue-copper site is remarkable. This is most clearly expressed by the relatively intense absorption of the oxidized protein around 630 nm. This property reflects the strongly covalent character of the Cu–S(cysteine) bond. Although the blue-copper site has been the subject of many extensive spectroscopic investigations and quantum-chemical calculations, consensus has not yet been reached with regard to the quantitative description of the molecular orbital that is instrumental in electron transfer. This particularly applies to its delocalization over the copper-coordinated cysteine residue.

Figure 1 shows the copper site of azurin. Previous studies have revealed the delocalization of the unpaired electron of oxidized azurin over the two histidine ligands. Electron spin-echo envelope modulation (ESEEM) experiments at X band (9 GHz) on frozen solutions of azurin show modulations that derive from the remote nitrogen atoms N_ε of the histidine ligands (His117 and His46).[1–4] At W band (95 GHz) single crystals could be studied by electron spin echo (ESE) detected electron paramagnetic resonance (EPR). At this high frequency electron nuclear double resonance (ENDOR) and ESEEM studies on a single crystal of azurin allowed the determination of the complete hyperfine tensor of, respectively, the remote and the coordinating nitrogen atoms of the histidine residues.[2,5] The unpaired electron was found to be asymmetrically delocalized over the histidine residues, with about twice as much spin density on His117 as on His46. Quantum-chemical calculations of the nitrogen hyperfine tensors on a truncated model of the copper site reproduced the observed asymmetry, albeit not quantitatively.[6–8] At the same time, however, these quantum-chemical calculations disagreed with respect to the delocalization of the unpaired electron over the copper and the sulfur

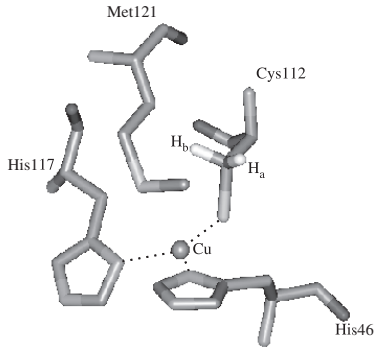

Figure 1. The copper site of azurin. The copper atom is bound strongly to three donor sites (N_δ of histidines 46 and 117 and S_γ of cysteine 112 with distances to copper of 2.11, 2.03, and 2.25 Å, respectively. The Cys-βHs H_a and H_b are also shown.

[a] *Dr. M. Fittipaldi, Dr. M. Huber, Prof. E. J. J. Groenen*
Department of Molecular Physics, Huygens Laboratory
Leiden University, P.O. Box 9504, 2300 RA Leiden (The Netherlands)
Fax: (+31) 71-5275936
E-mail: mat@molphys.leidenuniv.nl

[b] *G. C. M. Warmerdam, Dr. E. C. de Waal, Prof. G. W. Canters*
Gorlaeus Laboratories, Metallo Protein Group, Leiden University
P.O. Box 9502, 2300 RA Leiden (The Netherlands)

[c] *Dr. D. Cavazzini, Prof. G. L. Rossi*
Department of Biochemistry and Molecular Biology, University of Parma
Parco Area delle Scienze 23A, 43100 Parma (Italy)

atoms, with Mulliken spin densities ranging from 44% on Cu and 45% on S [6] to 27% on Cu and 61% on S.[8] For other blue-copper proteins calculations showed even larger variations. Among these, for plastocyanin the calculated copper 3d versus sulfur 3p character of the singly occupied molecular orbital (SOMO) of the oxidized protein ranged from 40/36% [9] to 81/17%.[10]

The hyperfine interaction of the unpaired electron with the nuclear spin of the protons bound to the C_β atom of cysteine (Cys-βHs) provides a measure of the copper–cysteine ligation. The isotropic hyperfine interaction of Cys-βHs has been investigated by Q-band (35 GHz) ENDOR on frozen solutions[11] and by 800 MHz ^{1}H NMR on liquid solutions [12] of blue-copper proteins. The isotropic proton hyperfine interaction is on the order of 20 MHz, but results are controversial. For azurin, the isotropic hyperfine interaction derived from the two experiments is quantitatively different. The NMR study indicates near equivalence of both Cys-βHs, while ENDOR indicates substantial inequivalence. As yet, complete hyperfine tensors of the Cys-βHs have not been determined. To determine the hyperfine tensors of the Cys-βHs, we performed 95 GHz pulsed ^{2}H ENDOR experiments on single crystals of an isotopomer of azurin from *Pseudomonas aeruginosa*, D-Az, in which the two Cys-βHs of the Cys 112 ligand have been replaced by deuterium. We chose to study D-Az instead of wild-type azurin because the ^{2}H ENDOR frequencies for this protein in principle enable the determination of the deuterium nuclear-quadrupole tensors (besides the hyperfine tensors). The quadrupole tensors provide the orientation of the C–D(H) bonds in the copper site, which gives information required for a quantitative interpretation of the hyperfine tensors. We report ^{2}H ENDOR spectra for many orientations of the magnetic field in the principal axes system of the *g*-tensor for one of the protein molecules in the unit cell. Analysis of the spectra was complicated by the fact that ENDOR linewidths, hyperfine anisotropy, and nuclear–quadrupole interaction are of the same order of magnitude. Nevertheless, based on some plausible assumptions, we were able to interpret the ENDOR data in terms of the spin-density delocalization over the copper-bound cysteine residue. About 45% of the spin density in the paramagnetic site can be attributed to copper-centered orbitals and 30% to sulfur-centered orbitals.

Results

To prepare for the ENDOR study, a complete orientational EPR study was performed on the single crystal of D-Az, following procedures outlined previously.[13] From this study the orientation in the laboratory frame of the *g*-tensor principal axes systems was obtained for all 16 azurin molecules in the unit cell (see Experimental Section). One of these molecules was selected for the ENDOR study, and Figure 2 shows a 95 GHz ^{2}H Mims-ENDOR spectrum. This spectrum was acquired with the direction of the external field $\vec{B}_0$ parallel to the *z* axis of the *g*-tensor of this molecule and at the EPR resonance field for this orientation of 2.9857 T. Two ENDOR signals are observed symmetrically displaced around the deuterium Zeeman frequency

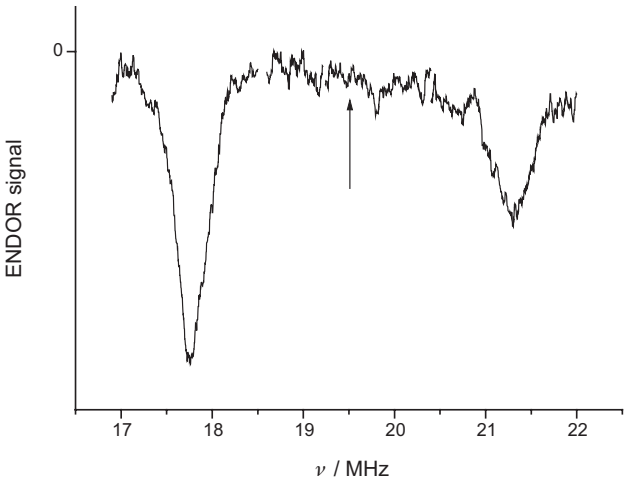

Figure 2. The ^{2}H Mims-ENDOR spectrum at 95 GHz of the D-Az single crystal for $\vec{B}_0$ parallel to the *z* axis of the *g*-tensor of one of the molecules in the unit cell ($B_0 = 2.9857$ T). The position of the arrow corresponds to the ^{2}H Zeeman frequency. The spectrum is composed of three spectra acquired by sweeping the frequency of the radiowaves continuously in three consecutive intervals. The intensity of the ENDOR signals above and below the Zeeman frequency can not be quantitatively compared.

of $\nu_Z = 19.51$ MHz for a magnetic field of 2.9857 T. Such ENDOR spectra were measured for many orientations of $\vec{B}_0$ with respect to the crystal by systematically varying the direction of $\vec{B}_0$ in the principal planes of the *g*-tensor of the molecule while adapting the magnitude of the magnetic field, calculated according to Equation (1) to remain in resonance with the corresponding EPR transition:

$$B_{res} = \frac{h\nu}{\beta_e \left[\sum_i (g_{ii} \cos \phi_i)^2\right]^{1/2}} \quad (1)$$

where $i = x, y, z$, h is the Planck constant, ν the frequency of the microwave radiation, β_e the Bohr magneton, and ϕ_i the angle between the principal *i* axis of the *g*-tensor of the molecule and the direction of $\vec{B}_0$. For the majority of the field directions we measured the ENDOR spectra only for frequencies smaller than the nuclear Zeeman frequency. The ENDOR frequencies above the nuclear Zeeman frequency have the same absolute displacement with respect to the Zeeman frequency and do not contain new information. Figure 3 shows the dependence of the ENDOR spectra on the orientation of the external magnetic field in the three principal planes of the *g*-tensor. For each orientation of $\vec{B}_0$ one broad ENDOR signal was observed, which sometimes reveals unresolved structure.

Figure 4 shows the 9 GHz Davies-ENDOR spectrum of a frozen solution of D-Az and of azurin acquired at a magnetic field of 0.32 T while sweeping the radiowave frequency from 1.5 to 31.5 MHz. A series of ENDOR spectra were acquired at different field positions in the EPR spectrum.

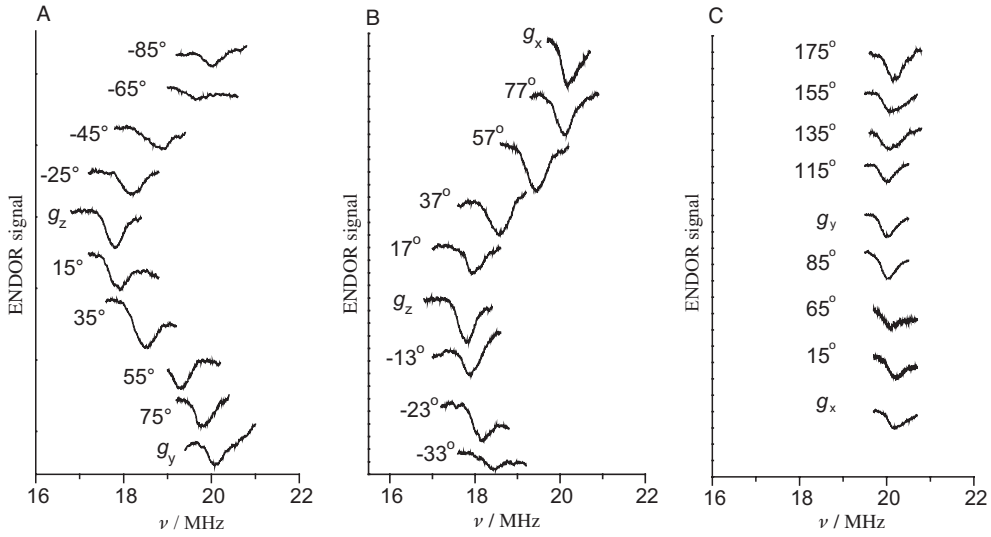

Figure 3. The ^{2}H Mims-ENDOR spectra at 95 GHz of the D-Az single crystal for various orientations of $\vec{B}_0$ in the three principal planes of the *g*-tensor of one of the molecules in the unit cell. The *yz* principal plane is shown in A), the *xz* principal plane in B), and the *xy* principal plane in C). For each orientation the part of the ENDOR spectrum below the Zeeman frequency is shown. Only parts of the orientations for which spectra have been measured are shown.

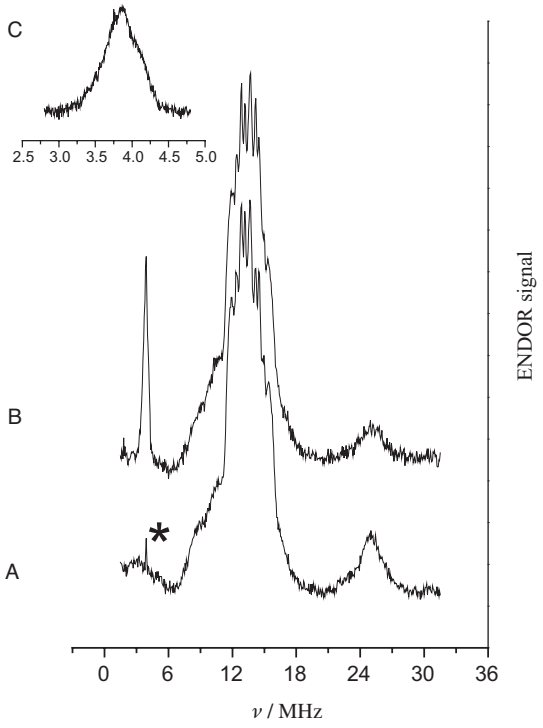

Figure 4. Davies ENDOR spectra at 9 GHz and $B_0 = 0.32$ T of frozen solutions of A) azurin, B) D-Az, and C) D-Az, acquired with a higher rf resolution. In spectrum (A) the asterisk indicates an artifact of the spectrometer.

Data Analysis

First consider the X-band ENDOR spectra of frozen solutions of undeuterated azurin represented in Figure 4, which provide us with a starting point for the analysis of the W-band ENDOR spectra of the single crystal of D-Az. The spectrum of azurin (Figure 4A) shows, besides a broad, structured band around 14 MHz, the ^{1}H nuclear Zeeman frequency, two broad signals around 3 and 25 MHz. These derive from the Cys-βHs, the hyperfine interactions of which are known to be on the order of 20 MHz.[11,12,14] Both nuclei contribute to the signal below and above the Zeeman frequency. The position of the ENDOR signals varies only a little with the magnetic field, that is, when selecting molecules differently oriented with respect to this field, which indicates that the hyperfine interaction is largely isotropic.

A proton hyperfine interaction of 20 MHz translates to a value of about 3 MHz for deuterium ($g_H/g_D \approx 6.5$). Indeed, in combination with the ^{2}H nuclear Zeeman frequency (2.1 MHz), an ENDOR signal is expected for D-Az at about 3.6 MHz, as seen in Figure 4B (the corresponding signal below the nuclear Zeeman frequency ends up very close to zero). As mentioned in the Experimental Section, isotopic substitution is not complete, and hence a residual proton ENDOR signal is seen at 25 MHz in Figure 4B. The narrow ^{2}H ENDOR signal reveals a shoulder, which reflects the contribution of two deuterium nuclei and appears more clearly in Figure 4C. For deuterium ($I = 1$), besides the anisotropic hyperfine interaction also the nuclear-quadrupole interaction contributes to the linewidth. From the comparison of the widths of the ^{1}H ENDOR lines (2.5 MHz, corresponding to $\approx$ 400 kHz for ^{2}H) and the ^{2}H ENDOR lines (600 kHz), we estimate the nuclear-quadrupole interaction to be at most 200 kHz.

The analysis of the X-band ENDOR data reveals that the hyperfine interaction and the nuclear-quadrupole interaction are smaller than the ^{2}H nuclear Zeeman frequency at W-band (19.6 MHz at 3 T). As a result, the ^{2}H ENDOR spectra of the single crystal of D-Az at W-band show signals symmetrically displaced around the nuclear Zeeman frequency (Figure 2), which means that we can restrict our analysis to the part of the ENDOR spectrum at and below (or above) the Zeeman frequency. Four transitions are expected to contribute to this part of the spectrum, two for each nucleus corresponding to the nuclear-spin transitions in one electron-spin manifold split by the nuclear-quadrupole interaction (Figure 5). To calculate the frequency of these transitions we must consider the spin Hamiltonian. At the microwave frequency of 95 GHz, mixing of the electron-spin levels can clearly be neglected and the spin Hamiltonian can be written as the sum of an electronic and a nuclear part. The nuclear-spin Hamiltonian for each deuterium [see Eq. (2)] includes the nuclear-Zeeman, hyperfine, and nuclear-quadrupole interactions:

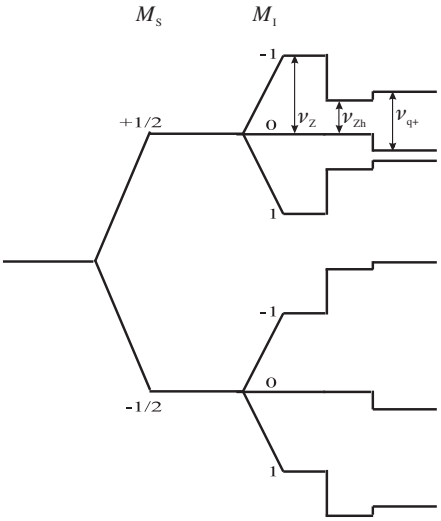

Figure 5. Energy-level scheme for a system with $S = {}^1/_2$ and $I = 1$, and $A_{iso} > 0$. The frequencies ν_Z, ν_{Zh}, and ν_{q+} are indicated.

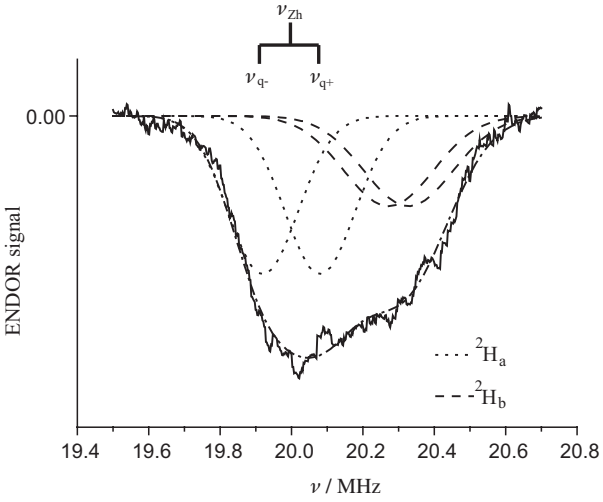

Figure 6. Illustration of the decomposition of a ^{2}H ENDOR spectrum at 95 GHz of the D-Az single crystal. ——: experimental spectrum acquired with $\vec{B}_0$ in *xy* principal plane of the *g*-tensor, making an angle of 145° with respect to the g_x axis. Pairs of Gaussian lines are symmetrically displaced with respect to ν_{Zh} and centered around ν_{q-} and ν_{q+}: ••••• for ^2H_a, ----- for ^2H_b. For this orientation the absolute value of the quadrupole splitting of ^2H_a is larger than that of ^2H_b. Position, intensity, and width of the lines were determined from a fit to the experimental spectrum. –•–•: sum of the four Gaussian lines.

$$H_n = -g(^2\mathrm{H})\beta_n \vec{I}\cdot\vec{B}_0 + M_S \frac{1}{g}\vec{I}\cdot\mathbf{g}\cdot\mathbf{A}\cdot\vec{I} + \vec{I}\cdot\mathbf{Q}\cdot\vec{I} \qquad (2)$$

where $g(^2\mathrm{H})$ is the nuclear *g*-factor of deuterium, β_n is the nuclear Bohr magneton, $\vec{I}$ is the nuclear-spin angular-momentum operator, M_S is the expectation value of the electron-spin angular-momentum operator ($\pm {}^1/_2$), **g** is the *g*-tensor, $\vec{I}$ is the unit vector which defines the orientation of $\vec{B}_0$ in the *g*-tensor principal axes system, *g* is equal to $(\vec{I}\cdot\mathbf{g}\cdot\mathbf{g}\cdot\vec{I})^{1/2}$, **A** is the hyperfine tensor, and **Q** is the nuclear-quadrupole tensor.

For each orientation of the magnetic field with respect to the crystal of D-Az, one broad ENDOR signal is observed below the ^{2}H Zeeman frequency (Figure 3), the linewidth of which varies from 350 to 550 kHz. To analyze the orientation dependence of the ENDOR signals in terms of hyperfine and nuclear-quadrupole tensors, the ENDOR frequencies for the two deuterium nuclei must be extracted from the broad ENDOR signal observed at each field orientation. To do so, we modeled the ENDOR signal as the sum of four Gaussians (Figure 6). For each nucleus, two Gaussians of equal intensity and width were taken centered at frequencies ν_{q-} and ν_{q+} positioned symmetrically around ν_{Zh}, which corresponds to the frequency in the absence of the quadrupole interaction (Figure 6). To calculate the quadrupole shift ($\nu_{q+} - \nu_{Zh}$) for both nuclei for each orientation of the magnetic field we needed only one parameter, say $Q_{z'z'}$. This results from the fact that we took the quadrupole interaction to be equal for both deuterium nuclei and that the electric-field gradient at the deuterium nuclei is determined by the symmetry of the chemical bond and, consequently, axially symmetric with respect to the main principal axis *z*′, which is along the direction of the respective C–D bonds. We fixed these directions on the basis of the X-ray structure (see Experimental Section). For each orientation of the magnetic field and for each deuterium nucleus, we calculated $\nu_{q\pm}$ by applying first-order perturbation theory to the eigenstates of the nuclear Zeeman interaction. Besides the intensity and the width of the Gaussians and the $Q_{z'z'}$ parameter, two more parameters ν_{Zh} for both deuterium nuclei, show up in the fit of the ENDOR signal for each orientation of the magnetic field. The best fits were obtained for $|Q_{z'z'}| = 107 \pm 20$ kHz and $|Q_{x'x'}| = |Q_{y'y'}| = 53.5 \pm 10$ kHz. The integrated intensities of the ^2H_a and ^2H_b signals are different, and the ratio of these intensities varies with the orientation of the magnetic field, which are observations that are not understood. For each orientation we obtained from the fit the frequencies ν_{Zh} for both deuterium nuclei. These frequencies, corrected for the Zeeman contribution, are represented in Figure 7. Because of the distinct orientations of the quadrupole *z*′ axes of both deuterium nuclei, the assignment of the ν_{Zh} values to the respective nuclei is unambiguous for many orientations of the magnetic field. For some orientations, particularly in the *yz* plane, a good fit was also obtained on interchanging the assignment of ν_{Zh} to the two deuterium nuclei. This ambiguity is resolved in the next step of the data analysis, in which the hyperfine tensors are determined. The frequencies ν_{Zh} of each nucleus as a function of the orientation of the magnetic field were fitted against the first two terms of the nuclear-spin Hamiltonian in Equation (2). Comparison of the quality of the fits for the different combinations of ν_{Zh} in the three principal planes indicated the proper assignment. At the same time, from the best fit for each nucleus, the hyperfine tensors of the two deuterium nuclei were obtained (Table 1). The results of the fits are shown in Figure 7. The absolute value of the isotropic hyperfine interaction is 3.2 MHz for both deuterium nuclei.

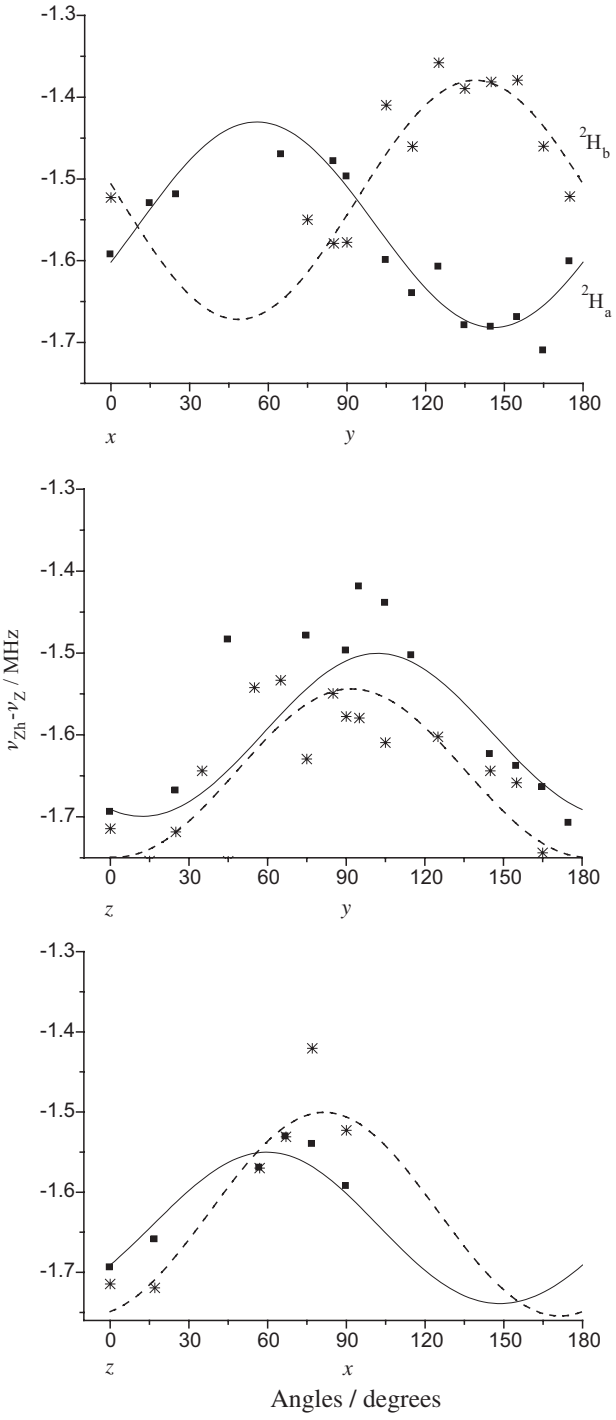

Figure 7. Orientation dependence of the frequencies ν_{Zh} (corrected for the nuclear Zeeman interaction) for the two deuterium atoms (■ = ^2H_a, * = ^2H_b) in the three principal planes. Solid and dashed lines: fits against the first two terms of Equation (2).

Discussion

From the pulsed ENDOR study at 95 GHz of single crystals of D-Az the complete hyperfine tensors of the deuterium atoms bound to the C_β atom of Cys112 (Cys-βDs) have been obtained. The analysis of the ENDOR bands was complicated by the unresolved quadrupole interaction and by the fact that the hyperfine interaction of both deuterium nuclei is largely isotropic and of similar magnitude. From a Gaussian deconvolution of the ENDOR bands based on the plausible assumption that the nuclear-quadrupole tensors are axial with their main axis along the respective carbon–deuterium bonds (the direction of which was constructed from the azurin structure as determined from X-ray diffraction data), quadrupole principal values of ± 107, ∓ 53.5, and ∓ 53.5 kHz were found. These values are in line with literature data for deuterium in carbon–deuterium bonds (accidentally equivalent to those reported for deuterated pyridine).[15] This observation supports the deconvolution procedure, and thereby the derived hyperfine tensors.

For the Cys-βDs an isotropic hyperfine interaction A_{iso} of 3.2 MHz has been obtained. In terms of hydrogen, which facilitates comparison with the literature, this value corresponds to 20.8 MHz. This Cys-βH isotropic hyperfine interaction yields an estimate of 1.5% for the spin density on each hydrogen atom (unit spin density in a hydrogen 1s orbital corresponds to an A_{iso} of 1420 MHz). The isotropic hyperfine interaction of both hydrogen atoms is the same within experimental uncertainty (± 0.2 MHz). From their ^{1}H NMR study at 800 MHz on azurin,[12] Bertini et al. obtained A_{iso} values of 27 and 28 MHz for the Cys-βHs, indeed about the same but 30% higher than our result. These values were derived from an extremely broad NMR line (1400 ppm FWHM), which was constructed from saturation-transfer experiments on a 50/50 mixture of oxidized and reduced protein. In a 95 GHz ENDOR spectrum at g_y of a frozen solution of wild-type azurin, Epel et al.[14] observed an unresolved proton ENDOR line corresponding to a hyperfine coupling of 22.2 MHz for the Cys-βHs, which is about 10% larger than our average coupling at g_y. In a 35 GHz ENDOR spectrum at g_z of a frozen solution of wild-type azurin, Werst et al.[11] observed a proton ENDOR line shifted by 10.3 MHz with respect to the proton Zeeman frequency. This line had a width of 5 MHz, probably determined by strain-induced inhomogeneity, and showed a slight structure on reduction of the amplitude of the field modulation. The authors concluded that the line reflects contributions of the two Cys-βHs, to which they assigned isotropic hyperfine couplings of 18 and 23 MHz. Such a difference is not compatible with the width of the ENDOR lines in the present study, and our analysis even reveals the near equivalence of both proton hyperfine interactions. Our value of 20.8 MHz is consistent with the ENDOR shift corresponding to the maximum of the line observed in the spectrum at 35 GHz.

The magnitude of A_{iso} [see Eq. (3)] is related to the spin density ρ_S on sulfur and the dihedral angle θ between the p orbital on S and the C_β–^{2}H bond:[14]

$$A_{iso} = \left(\cos^2\theta + \frac{C}{B}\right) B\rho_S \qquad (3)$$

where B is the contribution to A_{iso} from hyperconjugation and C accounts for the contribution from other mechanisms such as spin polarization. In the literature, values of these constants for protons bound to C_β have been reported, for B in the range of 80 to 100 MHz [16] and for C/B in the range of 0 to

Table 1. Hyperfine tensors of the two deuterium nuclei as obtained from the fit of the ν_{Zh} of each nucleus against the first two terms of the nuclear-spin Hamiltonian in Equation (2). The anisotropic hyperfine tensors are represented in the *g*-tensor reference frame (*x*, *y*, *z*). The values in parentheses indicate the asymptotic standard deviation of each element. The principal axes system of the hyperfine tensors is indicated by (x'', y'', z''). We have taken A_{iso} to be positive.

	A_{iso}/h [MHz]	$A_{x''x''}/h$ [MHz]	$A_{y''y''}/h$ [MHz]	$A_{z''z''}/h$ [MHz]	A_{aniso}/h [MHz]		
^2H_a	3.2	0.35	−0.01	−0.34	0.00 (0.04)	−0.23 (0.02)	−0.17 (0.05)
					−0.23 (0.02)	−0.18 (0.04)	0.08 (0.03)
					−0.17 (0.05)	0.08 (0.03)	0.18 (0.04)
^2H_b	3.2	0.31	0.13	−0.44	−0.19 (0.09)	0.29 (0.06)	−0.07 (0.09)
					0.29 (0.06)	−0.11 (0.08)	0.01 (0.04)
					−0.07 (0.09)	0.01 (0.04)	0.30 (0.08)

0.2.[11] The angle θ depends on the choice of the orientation of the p orbital that we use to model the spin density on sulfur. If we take this p orbital as p_y (in the reference frame *X*, *Y*, *Z* where Cu is at the origin, the sulfur atom of the cysteine residue on the negative *X* axis, and the copper-coordinating nitrogen atoms equidistant to the *XY* plane with $Z<0$) and combine its direction with the direction of the constructed C_β—^2H bonds, the angle θ becomes 40° and 159° (21°) for the respective deuterium atoms. The experimental value of A_{iso} is the same for both deuterium atoms, so, assuming that Equation (3) applies, the θ values should be the same. The difference probably derives from the simplicity of the model of the spin density on sulfur and the fact that Equation (3) is only approximately valid for the present configuration. From $\theta=30°$ and taking into account the uncertainty in the parameters *B* and *C*, we estimate ρ_S to be 30 ± 10%.

The anisotropy of the hyperfine interaction of the Cys-βDs amounts to at most 15%. Although small, the analysis of the anisotropic hyperfine tensor of each deuterium atom is of importance because it will provide insight into the electron-spin density distribution over copper and the cysteine ligand. The anisotropic hyperfine interaction is proportional to the spin density and inversely proportional to the third power of the distance between electron-spin density and nucleus. The analysis is difficult because even in the simplest model we have to consider contributions to the dipolar interaction of electron-spin density on four nuclei: S_γ and C_β of Cys112, Cu, and the other ^2H. The contributions of the spin density on these four nuclei are of the same order of magnitude: the C_β and the other ^2H carry little spin density but are close, while S_γ and the Cu are further away but carry much more spin density. The contribution of the spin density on the two copper-coordinating nitrogen atoms (4.9 and 9.4% [5]) to the deuterium hyperfine interaction can be neglected because it is estimated to be smaller than 10 kHz as a result of the large distance (ca. 4.7 Å) to the deuterium atoms. A preliminary analysis [17] of the anisotropic hyperfine tensor of ^2H_a (Table 1) taking into account the contributions of spin density in atomic orbitals centered on the four nuclei and spin densities of 30% on S_γ and 1.5% on ^2H indicates a spin density of about 45% on Cu. Summing up the spin densities on Cu, S_γ, and N_δ we then find about 0.9, that is, close to 1, which may provide confidence in the derived values of the spin densities. However, caution is needed because a similar analysis based on the tensor of ^2H_b failed, possibly because of the relatively large uncertainty in the elements of this tensor.

The present description of the hyperfine tensors of the Cys-βDs based on the simplest atomic-orbital spin model results in an estimate of the electron-spin density of 45 and 30% on the copper and cysteine sulfur atoms, respectively. Previously, a similarly simple analysis of the hyperfine tensors of the remote nitrogen atoms of the histidine residues indicated that about 15% spin density involves orbitals centered on the coordinating nitrogen atoms while virtually all other spin density is around copper and sulfur in the ratio 3:2.[5] Both studies thus yield qualitatively consistent results. On the other hand, an ab initio quantum-chemical study on a truncated model of the copper site of oxidized azurin resulted in a wavefunction of the unpaired electron that reproduced the *g*-tensor experimentally observed for azurin, and corresponds to respective Mulliken spin densities of 35 and 59% on the copper and cysteine sulfur atoms.[7] In other words, the calculated spin-density distribution deviates considerably from the experimental one, whereas the deviation of the g_z value from the free-electron *g* value, which is largely determined by the spin density on the heavy atoms copper and sulfur, is reproduced. We conclude that, although an impressive set of magnetic tensors is available from EPR/ENDOR studies, still more experimental and theoretical work is needed to arrive at a consistent picture of the spin-density distribution in the copper site.

Conclusions

A 95 GHz pulsed ^2H ENDOR study has been performed on single crystals of azurin deuterated at the C_β position of the copper-coordinating cysteine 112. From the preliminary analysis of the ENDOR spectra we derived that about 45% of the spin density in the paramagnetic site may be attributed to copper-centered orbitals and 30% to sulfur-centered orbitals. The analysis was hampered by the fact that the ENDOR lines showed little structure and contain unresolved quadrupole broadening. In addition, the contributions of the two Cys-βDs were difficult to distinguish because of the largely isotropic nature of the hyperfine interactions and the equivalence of their isotropic hyperfine interactions. To improve the accuracy of the anisotropic hyperfine tensors of the Cys-βHs, we plan to study the ^1H ENDOR spectra of a single crystal of wild-type azurin in the near future. Combination of these data with the present results will enable us to separate hyperfine and quadrupole contributions experimentally, to determine the direction of the cysteine C_β–H bonds (instead of constructing those on

the basis of the X-ray structure), and in this way improve the accuracy of the anisotropic hyperfine tensors of the Cys-βHs.

For azurin, whose copper site is closest to a model blue-copper site, an impressive EPR data set is now available, which consists of the full *g*-tensor, partial knowledge of the copper hyperfine tensors, and full hyperfine tensors of the coordinating and remote nitrogen atoms of copper-coordinating histidines 117 and 46 and of the Cys-βHs. The challenge for quantum chemistry is to come up with a wavefunction of the unpaired electron that provides a consistent description of all these data. If such a wavefunction were available, a quantitative treatment of electron transfer would be within reach.

Experimental Section

The ENDOR experiments were performed at 1.2 K using a home-built 95 GHz pulsed EPR spectrometer [18] with a microwave bridge manufactured by the Department of Microwave Equipment for Millimeter Waveband ESR Spectroscopy in Donetsk, Ukraine. A Mims type of pulse sequence was applied. The three microwave pulses had a width of 90 ns each. The separation between the first and second microwave pulse was typically 200 ns, and that between the second and third pulse 100 μs. The width of the radiofrequency (rf) pulse, which is applied between the last two microwave pulses, was 96 μs. The repetition rate was 2 Hz. The acquisition of an ENDOR spectrum took 10–15 min.

The orientation in the laboratory frame of the *g*-tensor principal axes (*x*, *y*, *z*) systems of the molecules in the unit cell of the D-Az crystals was determined from an EPR study on the single crystal. Subsequently, the ENDOR experiments were performed on the same crystal for various orientations of the magnetic field with respect to the *g*-tensor frame of one molecule in the unit cell. In order to analyze and discuss the ENDOR data in the molecular frame, we need to know the orientation of the *g*-tensor axes system in the copper site. Here we made the plausible assumption that this orientation is the same for D-Az as for undeuterated azurin from *Pseudomonas aeruginosa*. For undeuterated azurin, the orientation of the principal *g* axes in the copper site was determined previously from an ESE-detected EPR study on a single crystal of azurin[13] and coupling of these EPR data with the protein structure as determined by X-ray diffraction[19] (PDB code: 4Azu). Consequently, directions defined relative to the laboratory frame can be translated into directions defined in the copper site and vice versa. For the analysis of the ENDOR measurement we make use of the position of the Cys-βHs (Ds) of the copper-bound cysteine. These positions were calculated by using the X-ray data and the program BABEL 1.6. We also measured the ENDOR spectra of the histidine remote nitrogen atoms for the present crystal for several orientations of the magnetic field in order to achieve consistency in the definition of the direction of the *g* axes with respect to previous experiments on azurin.[5]

Protein concentration in the solutions used for the 9 GHz ENDOR measurements was 1 mM. The pulsed ENDOR measurements on the frozen solution were performed on a 9 GHz ELEXSYS E 680 spectrometer (Bruker, Rheinstetten, Germany). The measurements were performed at 6 K. A Davies type of pulse sequence was applied. The three microwave pulses had widths of respectively 200, 100, and 200 ns. The separation between the first and second microwave pulse was 8.8 μs, and that between the second and third pulses 248 ns. The width of the radiofrequency pulse, which is applied between the first two microwave pulses, was 6.2 μs. The repetition rate was 43 Hz. The acquisition time for a spectrum from 1.5 to 31.5 MHz was 140 min.

The D-Az protein was obtained as previously described[20] except that plasmid pGK22 was used and cells were grown overnight and diluted (1/100) in LB medium (5 L) supplemented with ampicillin (100 $\mu g\,ml^{-1}$) and L-cysteine-3,3-d_2 (0.01 %, Cambridge Isotope Laboratories, Inc. cat. no. DLM-769). At the end of the exponential growth, cells were harvested by centrifugation and azurin was isolated as described previously.[21] Mass spectrometry showed that the degree of deuteration was 70 %.

Crystals were obtained under the following conditions: protein solution (2 μL, 15 $mg\,mL^{-1}$, 10 mM Hepes pH 7) were mixed with mother liquor (2 μL) containing ammonium sulfate (3.4 M), lithium nitrate (0.5 M), and sodium acetate (50 mM), pH 5.5, to form a sitting drop which was allowed to equilibrate with mother liquor (1 mL).

The space group of the D-Az crystal is $P2_12_12_1$. The unit cell dimensions are 47.5, 97.7, and 107.9 Å, similar to those of the ^{15}N-labeled azurin crystals studied previously.[5] The unit cell contains four asymmetric units with four molecules per asymmetric unit. The size of the crystal used in the EPR/ENDOR study was $0.3\times0.3\times0.1$ mm. The single crystal was mounted in a quartz tube with inner and outer diameters of 0.6 and 0.84 mm, respectively. The tube ends were sealed by wax.

Acknowledgements

We gratefully thank S. B. Orlinski for his assistance during the measurements. G.L.R. acknowledges financial support by the Ministero dell'Istruzione, dell'Universitá e della Ricerca (MIUR), Italy. This work has been performed under the auspices of the BIOMAC Research School of the Leiden and Delft Universities and was supported with financial aid by The Netherlands Organization for Scientific Research (NWO), Department Chemical Sciences (CW).

Keywords: azurin · copper · ENDOR spectroscopy · EPR spectroscopy · proteins

[1] W. B. Mims, J. L. Davis, J. Peisach, *Biophys. J.* **1984**, *45*, 755–766.
[2] J. W. A. Coremans, M. van Gastel, O. G. Poluektov, E. J. J. Groenen, T. den Blaauwen, G. van Pouderoyen, G. W. Canters, H. Nar, C. Hammam, A. Messerschmidt, *Chem. Phys. Lett.* **1995**, *235*, 202–210.
[3] V. Kofman, O. Farver, I. Pecht, D. Goldfarb, *J. Am. Chem. Soc.* **1996**, *118*, 1201–1206.
[4] M. van Gastel, J. W. A. Coremans, L. C. J. Jeuken, G. W. Canters, E. J. J. Groenen, *J. Phys. Chem. A.* **1998**, *102*, 4462–4470.
[5] J. W. A. Coremans, O. G. Poluektov, E. J. J. Groenen, G. W. Canters, H. Nar, A. Messerschmidt, *J. Am. Chem. Soc.* **1996**, *118*, 12141–12153.
[6] A. R. Jaszewski, J. Jezierska, *Chem. Phys. Lett.* **2001**, *343*, 571–580.
[7] M. van Gastel, J. W. A. Coremans, H. Sommerdijk, M. C. van Hemert, E. J. J. Groenen, *J. Am. Chem. Soc.* **2002**, *124*, 2035–2041.
[8] S. Moons, S. Patchkovskii, D. R. Salahub, *J. Mol. Struct. Theochem.* **2003**, *632*, 287–295.
[9] K. W. Penfield, A. A. Gewirth, E. I. Solomon, *J. Am. Chem. Soc.* **1985**, *107*, 4519–4529.
[10] K. Pierloot, J. O. A. De Kerpel, U. Ryde, M. H. M. Olsson, B. O. Roos, *J. Am. Chem. Soc.* **1998**, *120*, 13156–13166.
[11] M. M. Werst, C. E. Davoust, B. M. Hoffman, *J. Am. Chem. Soc.* **1991**, *113*, 1533–1538.
[12] I. Bertini, C. O. Fernandez, B. G. Karlsson, J. Leckner, C. Luchinat, B. G. Malmstrom, A. M. Nersissian, R. Pierattelli, E. Shipp, J. S. Valentine, A. J. Vila, *J. Am. Chem. Soc.* **2000**, *122*, 3701–3707.
[13] J. W. A. Coremans, O. G. Poluektov, E. J. J. Groenen, G. W. Canters, H. Nar, A. Messerschmidt, *J. Am. Chem. Soc.* **1994**, *116*, 3097–3101.

[14] B. Epel, C. S. Slutter, F. Neese, P. M. H. Kroneck, W. G. Zumft, I. Pecht, O. Farver, Y. Lu, D. Goldfarb, *J. Am. Chem. Soc.* **2002**, *124*, 8152 – 8162.
[15] W. J. Buma, E. J. J. Groenen, J. Schmidt, R. de Beer, *J. Chem. Phys.* **1989**, *91*, 6549 – 6565.
[16] W. Gordy in *Theory and Applications of Electron Spin Resonance*, Wiley, New York, 1980.
[17] M. Fittipaldi, *The Electronic Structure of Copper Sites in Proteins. A Pulsed and High-Field EPR Study*, Thesis, Leiden University, **2004**.
[18] J. A. J. M. Disselhorst, H. van der Meer, O. G. Poluektov, J. Schmidt, *J. Magn. Reson. Ser A* **1995**, *115*, 183 – 188.
[19] H. Nar, A. Messerschmidt, R. Huber, M. van de Kamp, G. W. Canters, *J. Mol. Biol.* **1991**, *221*, 765 – 772.
[20] I. M. C. van Amsterdam, M. Ubbink, L. J. C. Jeuken, M. P. Verbeet, O. Einsle, A. Messerschmidt, G. W. Canters, *Chem. Eur. J.* **2001**, *7*, 2398 – 2406.
[21] M. van de Kamp, F. C. Hali, N. Rosato, A. F. Agro, G. W. Canters, *Biochim. Biophys. Acta* **1990**, *1019*, 283 – 292.

Received: October 10, 2005
Revised: February 28, 2006
Published online on May 9, 2006

